Journal of Zhejiang University-SCIENCE B (Biomedicine & Biotechnology) in press
www.jzus.zju.edu.cn; www.springer.com/journal/11585
E-mail: jzus_b@zju.edu.cn

Research Article

https://doi.org/10.1631/jzus.B2500233

Type 2 inflammation accelerates CD4$^+$ T-Cell senescence in asthma

Huan LIU[1,2], Zemin LI[1,2], Yongchang SUN[1,2], Abudureyimujiang AILI[3]✉, Chun CHANG[1,2]✉

[1]*Department of Respiratory and Critical Care Medicine, Peking University Third Hospital, Beijing 100083, China*
[2]*Research Center for Chronic Airway Diseases, Peking University Health Science Center, Beijing 100083, China*
[3]*Department of Medical Oncology and Radiation Sickness, Peking University Third Hospital, Beijing 100083, China*

Abstract: Asthma is a complex and chronic inflammatory airway disease associated with the abnormal activation of immune cells. T-cell senescence is linked to immune dysfunction and persistent inflammation, but the relationship between asthma and T-cell senescence remains unexplored. This study reveals significantly higher percentages of cluster of differentiation 4-positive (CD4$^+$) senescent T-cells (Tsens) in asthma patients than in healthy controls, while CD8$^+$ Tsen percentages do not appear to increase. CD4$^+$ Tsen percentages in both the blood and sputum are positively correlated with fractional exhaled nitric oxide (FeNO) values, eosinophil abundance, and T helper type 2 (Th2) cell abundance in the blood. The clinical manifestations of asthma were recreated in a house dust-mite (HDM)-induced mouse model. In HDM-exposed mice, CD4$^+$ Tsen percentages were also elevated in the lungs. To counteract T-cell senescence, therapeutic interventions, including interleukin-4 (IL-4) antibodies and dexamethasone, were administered to the mice. IL-4 neutralization reduced CD4$^+$ Tsen percentages and inhibited p38 mitogen-activated protein kinase (MAPK) activation. Adoptive transfer of senescent CD4$^+$ T cells did not induce spontaneous asthma in phosphate-buffered saline (PBS)-treated mice but exacerbated type 2 inflammation in HDM-treated mice. Our study revealed a significant increase in senescent CD4$^+$ T-cell abundance (CD57$^+$CD28$^-$) in asthma patients and suggests that type 2 inflammation drives CD4$^+$ T-cell senescence in asthma. Furthermore, adoptive transfer of senescent CD4$^+$ T cells appears to exacerbate type 2 inflammation.

Key words: Asthma; Cellular senescence; T cells; Inflammation

unedited

1 Introduction

Asthma, a chronic inflammatory disease, is characterized by airway hyperresponsiveness and reversible airway obstruction (Huang et al., 2019). The Global Burden of Disease study identified asthma as one of the most prevalent chronic respiratory diseases globally (Collaborators, 2020). Type 2 asthma is the most common phenotype and is typically associated with allergen sensitivity and T helper cell type 2 (Th2)-mediated immunity involving immunoglobulin E (IgE) (Ödling et al., 2018; Hammad and Lambrecht, 2021). Cell senescence, a state triggered by stress-induced damage and some physiological processes, is characterized by prolonged, often irreversible, cell-cycle arrest (Gorgoulis et al., 2019). Senescent human T cells lose expression of costimulatory molecules, such as CD27 and CD28, while the expression of terminal differentiation markers, such as CD57, is upregulated (Mittelbrunn and Kroemer, 2021). Compared with nonsenescent cells, senescent cells display distinct characteristics, including increased senescence-associated β galactosidase (SA-β-Gal) activity (Childs et al., 2017), a higher percentage of killer-cell lectin-like receptor G1 (KLRG1) (Akbar et al., 2016) and programmed cell-death protein 1 (PD-1) expression (Wang et al., 2022), as well as elevated levels of p16 (Wood et al., 2016) and p21 (Sturmlechner et al., 2021).

Cellular senescence is associated with chronic low-grade inflammation and is observed in several inflammatory diseases, including chronic obstructive pulmonary disease (COPD), renal disease, obesity-related

✉ Chun CHANG, changc@bjmu.edu.cn; Abudureyimujiang AILI, aa@bjmu.edu.cn
Chun CHANG, https://orcid.org/0000-0003-1362-5950; Abudureyimujiang AILI, https://orcid.org/0000-0002-6893-5561
Huan LIU, https://orcid.org/0000-0003-4487-9742
Received May 6, 2025; Revision accepted Aug. 13, 2025;
Crosschecked xxx. xx, 20xx; Published online xxx. xx, 20xx

© Zhejiang University Press 2025

metabolic syndrome, type I and II diabetes, atherosclerosis, and Alzheimer's disease (Childs et al., 2015; López-Otín et al., 2023; Devulder, 2024). Systemic elevation of inflammatory mediator levels may contribute to early immunosenescence (Madruga et al., 2024). Previous studies have shown that airway smooth muscle cells in the lungs of elderly asthma patients exhibit increased expression of senescence markers, including p53, p21, and several senescence-associated secretory phenotype (SASP) components (Aghali et al., 2022). Additionally, increased cellular senescence has been observed in bronchial fibroblasts and myofibroblasts in the lungs of asthma patients(Schafer et al., 2017). Some immune cells, including macrophages, T cells, and B cells, may undergo senescence due to chronic inflammation and oxidative stress (Wang et al., 2020; Wan et al., 2023). Several factors such as acute and chronic infection, cellular attrition, insufficient replacement of naïve cells, and proliferative stress on naïve T cells, make T cells particularly susceptible to senescence (Weyand et al., 2014). While the concept of T-cell senescence has been extensively studied in the context of viral infection and autoimmune disease, there are few studies on senescent T cells in asthma patients.

To investigate potential differences in T-cell senescence between asthma patients and healthy controls, we analyzed its occurrence in both human patients and a mouse model of asthma. We found that an increase in senescent $CD4^+$ T-cell abundance is a common feature of type 2 asthma. Furthermore, increased type 2 inflammation in asthma patients was positively correlated with the percentage of senescent $CD4^+$ T cells. In vivo studies demonstrated that inhibiting type 2 inflammatory pathways, either through IL-4 antibody neutralization or dexamethasone treatment, effectively prevents $CD4^+$ T-cell senescence and alleviates asthma-related pulmonary inflammation. Stimulation with IL-4 exacerbated the senescence of human $CD4^+$ T cells in vitro. In contrast, infusion of senescent $CD4^+$ T cells into healthy mice did not induce spontaneous asthma, but infusion into HDM-treated mice worsened type 2 inflammation.

unedited

2 Materials and methods

2.1 Study population

Peripheral blood samples were collected from 50 continuously enrolled patients diagnosed with chronic persistent asthma at the Third Hospital of Peking University and from 14 healthy controls. Age, sex, and body mass index (BMI) were matched between the asthma cohort and the healthy control group. In addition, 36 asthma patients and 8 healthy controls provided induced sputum samples. All enrolled patients met the diagnostic criteria for asthma established by the Global Initiative for Asthma (GINA) 2023. We excluded pregnant women and patients with: acute asthma exacerbation within the past four weeks; coexisting respiratory disease; severe cardiovascular, hepatic, or renal disease; rheumatoid immune disease; metabolic disease; malignant disease; and immunodeficiency or other major medical illness. The healthy controls had no history or symptoms of chronic respiratory disease, metabolism-related disease, allergic disease, or any other factors that might have influenced the study outcome. This study was approved by the Medical Science Research Ethics Committee of the Third Hospital of Peking University (Approval no. M2023075), and all participants provided written informed consent.

2.2 Classification of asthma subgroups

The patients were classified into different subgroups according to age: young (18–44 years old), middle-aged (45–60 years old), and elderly (≥60 years old), and BMI: (slim (<18.5 kg/m^2), normal (18.5–23.9 kg/m^2), and overweight (24.0–27.9 kg/m^2). Based on the age of first onset, patients were categorized into early-onset (< 40 years old) and late-onset (≥40 years old) groups. Based on the ratio of FEV_1/FVC in pulmonary function after bronchodilator inhalation, patients were classified into two subgroups: those with fixed airflow-limitation (forced expiratory volume in 1 s (FEV1) / forced vital capacity (FVC) < 0.7) and those without fixed airflow limitation (FEV1/FVC > 0.7). After we assessed their treatment information, patients were classified into subgroups for GINA stages 1-4 and GINA stage 5 (according to GINA2023). Low vs. high FeNO was

bounded by 20 ppb, the hypereosinophilic group vs. the hypoeosinophilic group were bounded by 150/μL of eosinophils, and high vs. low sputum eosinophils were bounded by 2% of the sputum eosinophil ratio.

2.3 Isolation of peripheral blood cells

Peripheral venous blood (2 mL) was collected in an ethylenediaminetetraacetic acid (EDTA) anticoagulant tube and subjected to separation into plasma and cells via centrifugation at 2000 ×*g* for 10 min. Red blood-cell lysis was performed using a red blood-cell lysing solution (Solarbio, China) according to the manufacturer's instructions. The remaining white blood cells were washed twice with phosphate-buffered saline (PBS) and suspended to a concentration of 1×10^7 cells/mL in PBS. We analyzed this cell suspension using flow cytometry.

2.4 Isolation of induced sputum cell

Induced sputum was obtained from participants following nebulized inhalation of 3% hypertonic saline. Sputum plugs were separated from saliva and were incubated with an equal volume of 0.4% dithiothreitol in a 37°C water bath with shaking, for 30 min. We stained the cells using Wright–Giemsa stain, and counted and sorted 200 inflammatory cells.

2.5 Quantification of plasma proinflammatory cytokines

According to the manufacturer's guidelines, we used a multiplexed microbead-based immunoassay system (LEGENDPlex™, Biolegend) to quantify the level of proinflammatory cytokines. A preformulated panel kit (Human Inflammation Panel 1) was used for quantification. Data were collected using CytoFLEX S Flow Cytometer (Beckman Coulter) and analyzed using proprietary data-analysis software (Biolegend).

2.6 Mouse model

All animal experiments were approved by the Institutional Animal Care and Use Committee of Peking University Health Science Center (No. PUIRB–LA2022692). The HDM-induced mouse model was established as previously described (Tibbitt et al., 2019). Additional details regarding the mouse model and animal experiments are provided in the supplementary methods. Mice aged 6–8 weeks were anesthetized with isoflurane and treated with 1 μg HDM in 40 mL PBS for intranasal sensitization on Day 0. Next, on Day 7, the mice received 10 μg intranasal HDM for 5 consecutive days. Finally, 4 days after the final stimulation (Day 11), the mice were sacrificed and their lungs and spleen were dissected for subsequent analysis.

For neutralization studies, the mice were given intraperitoneal injection of 7.5 mg/kg anti-IL-4 mAb 4 h prior to challenge on Days 7, 9, and 11. Some mice were given 2.5 mg/kg dexamethasone (DEX) via intraperitoneal injection on days 12 and 14.

For adoptive transfusion, we intravenously transferred 500,000 Dox-treated or PBS-treated mouse $CD4^+$ T cells into the mice with asthma on Days 7 and 11.

2.7 Airway-resistance analysis

We assessed mouse lungs using the flexiVent system (Scireq, Montreal, Canada), and recorded certain parameters, such as the total resistance of the respiratory system (Rrs), as per a previously described method (Kalidhindi et al., 2021). Next, we obtained a measure of airway responsiveness to nebulized methacholine using the forced oscillation technique, in which we delivered increasing concentrations of methacholine (0, 6, 12, 24, and 48 mg/mL) in PBS via an ultrasonic nebulizer.

2.8 Lung histological analysis

Dissected left lung tissue was fixed with 4% paraformaldehyde for 24 h, dehydrated with successive ethanol concentrations, and embedded in paraffin. Next, 6-μm sections were prepared and stained with hema-

Unedited

toxylin and eosin (HE) and periodic acid–Schiff (PAS) for assessment of goblet-cell hyperplasia. We obtained images using the 3D Histech digital scanner (Budapest, Hungary). Histological scoring of allergic pulmonary inflammation in the lungs was performed separately by two blinded observers; the final score was the average of the scores of the two observers. As in a previous study, the score was determined according to the cellular infiltration around blood vessels and airways, with 0 being the lowest and 4 being the highest (Nakagami et al., 2008). The PAS grading system has been described elsewhere (Zhang et al., 2023).

2.9 Single-cell dissociation of lung and spleen tissue

After dissecting the right lung tissue, we added collagenase type 4 and deoxyribonuclease I (Worthington-Biochem, Lakewood, NJ, USA) for digestion in the oscillating incubator at 37 °C for 40 min. The digested tissue was ground to a single-cell suspension with a 40-μm filter and subjected to red-blood-cell lysis. The spleen tissue was processed in a similar manner. The isolated cells were washed twice with PBS and suspended to a concentration of 1×10^7 cells/mL. The cells were appropriately stained and analyzed via flow cytometry.

2.10 Sorting and culture of cells

We isolated the $CD4^+$ T cells used in this study from the spleens of C57BL/6 wild-type mice using a $CD4^+$ T-cell isolation kit (19852RF, STEMCELL), and also isolated human peripheral blood mononuclear cells (PBMCs) using a $CD4^+$ T-cell isolation kit (17952RF, STEMCELL) according to the manufacturer's protocol. EDTA-anticoagulated blood from healthy volunteers was diluted 1:1 with PBS and subjected to density gradient centrifugation at 400*g* for 30 min at room temperature using Ficoll-Paque PREMIUM 1.073 (17-5446-52, GE Healthcare), with gradual acceleration and deceleration. $CD4^+$ T cells were cultured in Roswell Park Memorial Institute 1640 (RPMI 1640) medium (C11875500BT, Gibco) supplemented with 10% fetal calf serum (11560636, Gibco) and 1% penicillin/streptomycin (15070063, Gibco).

2.11 Flow cytometry

The procedures used to isolate peripheral blood cells and sputum cells are detailed in the supplementary methods, and all the antibodies included in the panels used in this study are listed in Supplementary Table S5. The gating strategy is shown in Figs. S1-S3. Data acquisition was performed using a CytoFLEX S flow cytometer (Beckman Coulter) and an ID7000™ Spectral Cell Analyzer. Flow-cytometry data were analyzed using FlowJo software (version 10).

2.12 Western blot

All proteins extracted from tissue were separated by sodium dodecyl sulfate–polyacrylamide gel electrophoresis (SDS‐PAGE) and transferred to polyvinylidene difluoride (PVDF) membrane (Millipore, Billerica, MA, USA). The membrane was incubated with 5% skim milk at room temperature (22 °C) for 1 h and then incubated with primary antibody overnight at 4 °C. Finally, it was incubated with goat anti-rabbit horseradish peroxidase immunoglobulin G at room temperature for 1 hour. Images were analyzed using ImageJ software.

2.13 Statistical Analysis

We analyzed differences between two groups using two-tailed Student's t test for parametric data or the Mann–Whitney test for nonparametric data. Differences in continuous variables among three groups were evaluated using one-way analysis of variance (ANOVA). Categorical data were analyzed using Pearson's Chi-square test (χ^2 test), and correlation analysis was performed using Spearman's rank correlation coefficient. $P < 0.05$ was considered to indicate statistical significance. All statistical analyses were performed with GraphPad Prism software (version 8).

unedited

3 Results

3.1 Clinical characteristics of asthma patients

The study included 50 asthma patients and 14 age-matched healthy controls, with some subjects providing induced sputum samples. The demographic and clinical characteristics of the participants are summarized in Tables 1 and S1. No significant differences in age, sex, body mass index (BMI), or smoking history were observed between the groups. The flow-cytometry results revealed that the percentage of Th2 cells in the blood of asthma patients was significantly greater than that in the control group, whereas the proportion of Th1 cells was lower (Table S2, Fig. S4). Additionally, the proportions of Th17 and Treg cells were elevated in the blood of asthma patients, but the Th17/Treg ratio was greater than that in the blood of healthy controls, suggesting that a Th17/Treg imbalance occurs in the peripheral blood of asthma patients. However, there were very few $CD4^+$ T cells in the sputum, and we observed no significant differences in Th2 cells or other T-cell subsets between patients and controls (Table S3). The proportions of all Th subgroups were analyzed by gating for $CD4^+$ T cells.

3.2 $CD4^+$ Tsen Percentages Increased in Asthma Patients

To mitigate the potential confounding effects of clinical characteristics such as age and BMI on Tsens, we matched these variables between asthma patients and healthy controls. Compared with the non-senescent $CD57^-CD28^+$ (Tn) subset, the $CD57^+CD28^-$ Tsen subset of $CD4^+$ or $CD8^+$ T cells presented greater SA-β-Gal activity (Fig. S5a). Moreover, the expression of p16 (Fig. S5b) and p21 (Fig. S5c) and the percentage of cells expressing KLRG1 (Fig. S5d), a marker of terminal differentiation, were significantly increased in Tsens in both asthma patients and controls. Among $CD4^+$ T cells, the percentage of PD-1-positive cells (Fig. S5e) was also significantly increased in Tsens, but this pattern was not observed in $CD8^+$ T cells. Notably, senescent $CD57^+CD28^-$ cells in both $CD4^+$ and $CD8^+$ T cell subsets consistently produced higher levels of IL-6 and IFN-γ compared to their non-senescent counterparts (Figs. S5f and S5g). In summary, the $CD57^+CD28^-$ T-cell subset from asthma patients exhibited common features of senescent cells, which may provide markers for detecting Tsens in asthma.

In the peripheral blood, we found no significant difference in the proportions of $CD4^+$ and $CD8^+$ T cells between the two groups (Fig. 1a). Flow cytometry revealed that both the $CD4^+$ and $CD8^+$ T cell populations contained senescent cells. Furthermore, the proportion of $CD4^+$ Tsens was significantly greater in asthma patients ((2.43±1.37) %) than in healthy controls ((1.43±0.65) %, $P < 0.05$; Fig. 1a). However, no significant difference in the proportion of $CD8^+$ Tsens was detected between asthma patients ((23.48 ± 6.42) %) and healthy controls (21.18% ± 4.16%; $p > 0.05$). We did not observe any differences in $CD4^+CD57^-CD28^+$ or $CD8^+CD57^-CD28^+$ non-senescent T cells between the two groups. The proportion of senescent $CD4^+$ T cells in the sputum of asthma patients was greater than that in the sputum of healthy controls (Fig. 1d), indicating that asthma patients had more senescent $CD4^+$ T cells in both the peripheral blood and the local airway. $CD4^+$ Tsens also showed potential as a distinguishing feature between individuals with and without asthma, with an area under the receiver operating characteristic curve of 0.716 ($p < 0.05$, Fig. 1b).

3.3 Differences in $CD4^+$ Tsen Abundance between Different Clinical Phenotypes of Asthma

To explore the relationships between $CD4^+$ Tsen abundance and different asthma phenotypes, we stratified patients according to various classification criteria (Figs. 1f-l). $CD4^+$ Tsen percentages were significantly elevated in patients with poorly controlled asthma (ACT < 20) compared with patients with well controlled asthma (ACT ≥ 20) (Fig. 1j). We also assessed various senescence-related proinflammatory cytokines in the peripheral blood (Table S4). The results revealed that the levels of IFN-γ, TNF-α, IL-1β, IL-6, IL-17A, IL-23, and IL-33 were significantly greater in asthma patients than in controls (Table S4, Fig. S6a). Furthermore, levels of the senescence-related cytokines IL-6 and IL-17A were significantly negatively correlated with ACT scores (Fig.

unedited

S6b), suggesting that poorer asthma control was associated with higher levels of SASP components such as IL-6 in the peripheral blood.

We also found that the percentage of $CD4^+$ Tsens was positively associated with age and BMI in asthma patients (Fig. 1c), and that elderly patients (≥ 60 years old) presented higher percentages of $CD4^+$ Tsens than younger patients did (18–44 years old, $p = 0.068$; Fig. 1f). However, no significant differences in $CD4^+$ Tsen abundance were found across subgroups delineated on the basis of sex or other factors.

3.4 $CD4^+$ Tsen Abundance was Positively Correlated with Type 2 Inflammation in Asthma

Most asthma patients present with type 2 inflammation, characterized by blood eosinophil numbers ≥ 150/μl, FeNO values ≥ 20 ppb, sputum eosinophil percentages ≥ 2%, and/or clinical allergen-driven asthma. We investigated the association between $CD4^+$ Tsen abundance and type 2 inflammation, and found that FeNO values were significantly positively correlated with the proportion of $CD4^+$ Tsens ($r = 0.378$, $p = 0.025$) and that the percentage of Th2 cells in the blood was also significantly positively correlated with the proportion of $CD4^+$ Tsens ($r = 0.288$, $p = 0.042$, Fig. 1c). However, no significant correlation was detected between the proportion of neutrophils in the sputum or Th17 cells in the blood and the proportion of $CD4^+$ Tsens in the blood (Fig. 1c). Moreover, we found significant positive correlations between $CD4^+$ Tsen abundance in the sputum and both the proportion and number of eosinophils in the peripheral blood (Fig. 1e). Correlation analysis suggested that $CD4^+$ abundance was positively correlated with type 2 inflammation in asthma patients. Subgroup analysis according to asthma endotype (Figs. 1m-p) further revealed that patients with FeNO ≥ 20 ppb had more $CD4^+$ Tsens (2.71% ± 1.33%) than those with FeNO < 20 ppb (1.58% ± 1.07%; $p = 0.0429$; Fig.1n), highlighting the importance of targeting type 2 inflammation in asthma treatment.

Unedited

3.5 $CD4^+$ Tsen Percentages were Significantly Elevated in Mice with HDM-Induced Asthma

We showed that $CD4^+$ Tsen abundance was significantly positively correlated with type 2 inflammation, but it remained unclear whether the observed increase in senescent cell abundance was directly caused by type 2 inflammation. To address this question, we used an HDM-induced mouse model of asthma, which is dominated by type 2 inflammation (Fig. S7a). Compared with control mice, HDM-treated mice presented significantly increased respiratory resistance (Rrs) following exposure to increasing concentrations of methacholine (Fig. 2a). Histological examination after H&E staining revealed more severe bronchial and perivascular inflammatory cell infiltration in the asthma group than in the control group (Fig. 2b). PAS staining further revealed significantly greater airway mucus hypersecretion in asthmatic mice (Fig. 2b). Since mouse T cells do not express the CD57 antigen, we used CD153 and PD-1 to characterize senescent T cells (Yoshida et al., 2020). CD153 (also known as TNFSF8 or CD40L ligand) is a membrane-binding protein that belongs to the tumour necrosis factor superfamily, is expressed on activated T cells, and is increasingly recognized as a marker of senescent cells (Yoshida, et al., 2020). Percentages of $CD4^+$ Tsens in the lungs and spleens of asthmatic mice were significantly greater than in the lungs and spleens of control mice (Fig. 2c). However, no significant difference in $CD8^+$ Tsen abundance was observed between the two groups (Fig. 2c). Compared with mouse non-senescent $CD4^+$ T cells ($CD153^-PD1^-$, Tn), senescent $CD4^+$ T cells ($CD153^+PD1^+$, Tsens) exhibited higher levels of SA-β-Gal and γ-H2AX (Figs. 2d and 2e). These findings suggest that the $CD4^+$ T-cell senescence phenotype observed in the mouse asthma model closely resembles that in humans.

3.6 IL-4 Antibody Treatment Decreased Senescent $CD4^+$ T-Cell Abundance in HDM-Treated Mice

To further explore the causal relationship between type 2 inflammation and $CD4^+$ T-cell senescence, we treated mice with HDM-induced asthma with monoclonal anti-IL-4 antibodies to neutralize IL-4, a key cytokine involved in type 2 inflammation, and dexamethasone, a nonspecific anti-inflammatory agent (Fig. S7b). Both treatments significantly reduced airway resistance (Fig. 3a) and decreased the proportion and number of eo-

sinophils, as well as the percentages of Th2 cells in the blood, bronchoalveolar lavage fluid (BALF), and lung tissue of asthmatic mice (Figs. 3b-f). In addition, these treatments alleviated lung inflammation and mucus hypersecretion (Figs. 3g-h). It is notable that treatment with either the anti-IL-4 antibody or dexamethasone significantly reduced the proportion of senescent $CD4^+$ T cells in the lungs and spleen (Fig. 3i) and reduced SA-β-gal activity in $CD4^+$ T cells in the lungs (Fig. 3j).

Recent studies have suggested that IL-4 activates multiple signal-transduction pathways, such as the STAT6 and p38 MAPK pathways, which are considered potential mechanisms for inducing cellular senescence (Min et al., 2022). We analyzed the phosphorylation of proteins involved in these signalling pathways in the lung tissue of HDM-treated mice and found that phosphorylation of STAT6 and p38 MAPK was significantly increased (Figs. 4a and 4b). However, in mice treated with the anti-IL-4 antibody, phosphorylation of p38 MAPK and total p38 MAPK was significantly reduced and phosphorylation of STAT6 remained unchanged (Figs. 4a and 4b). To verify the effects of IL-4, IL-5, and IL-13 on $CD4^+$ T cells *in vitro*, we isolated human $CD4^+$T cells and cultured them with various concentrations of IL-4, IL-5, and IL-13. SA-β-gal staining revealed that IL-4, IL-13, and high concentrations of IL-5 significantly increased SA-β-gal activity in $CD4^+$ T cells (Fig. 4c), suggesting that type 2 inflammatory cytokines can induce $CD4^+$ T-cell senescence. We investigated the mechanism of IL-4 in human peripheral-blood-derived $CD4^+$ T cells and found that IL-4 stimulation enhanced phosphorylation of p38 MAPK without affecting STAT6 phosphorylation (Figs. 4d and 4e). Flow-cytometry analysis revealed that the addition of the p38 MAPK inhibitor (SB202190) significantly reduced SA-β-gal activity compared to IL-4 stimulation alone (Fig. 4f).

3.7 Adoptive Transfer of Senescent $CD4^+$ T Cells Promoted Type 2 Inflammation

To investigate the role of senescent $CD4^+$ T cells in the pathogenesis of asthma, we performed adoptive transfer of senescent $CD4^+$ T cells into healthy or asthmatic mice (Fig. S7c). Since it is difficult to acquire sufficient numbers of senescent $CD4^+$ T cells from patients or asthmatic mice for adoptive transfer, we isolated $CD4^+$ T cells from the spleens of these mice and induced senescence with doxorubicin (Dox). We found that 50 nM Dox efficiently induced $CD4^+$ T-cell senescence, as evidenced by increased β-gal activity, induction of the $CD153^+PD1^+$ phenotype, and increased levels of p16 and γ-H2AX (Fig. 5a). These findings suggest that Dox-treated $CD4^+$ T cells exhibit phenotypic characteristics similar to those of senescent $CD4^+$ T cells. We then performed adoptive transfer of Dox-induced senescent $CD4^+$ T cells or control $CD4^+$ T cells into healthy mice. Mice that received senescent $CD4^+$ T cells exhibited increased proportions of senescent $CD4^+$ T cells in the lung and spleen, along with increased SA-β-gal activity in $CD4^+$ T cells in the lung (Figs. 5b and 5c). However, these mice did not exhibit increased airway resistance (Fig. 5d) or an elevated proportion of Th2 cells (Fig. 5g) or eosinophils in the lung (Fig. 5f), nor did they show significant mucus hypersecretion (Fig. 5i). Interestingly, there were significant increases in the abundance of eosinophils in the BALF (Fig. 5e) and in the infiltration of inflammatory cells into the lung (Fig. 5h). These results suggest that while adoptive transfer of senescent $CD4^+$ T cells does not induce spontaneous asthma in healthy mice, it does promote local inflammation in the lungs.

We also performed adoptive transfer of senescent $CD4^+$ T cells from HDM-treated mice (Fig. S7c). Mice that received these senescent $CD4^+$ T cells exhibited increased proportions of senescent $CD4^+$ T cells in the lung and spleen, as well as increased SA-β-gal activity in lung $CD4^+$ T cells (Fig. 6a). These mice also showed significant increases in airway resistance (Fig. 6b), eosinophil abundance, and Th2-cell abundance in the lung and BALF (Figs. 6c-f). Moreover, lung inflammation and mucus hypersecretion were significantly increased in these mice (Figs. 6g-h). These findings suggest that senescent $CD4^+$ T cells exacerbate type 2 inflammation in asthma through positive feedback mechanisms.

unedited

4 Discussion

T cells are crucial components of the immune system, and T-cell senescence is considered one of the key features of immune-system senescence (Soma and Nagata, 2022). Studies have shown that long-term chronic inflammation accelerates T-cell senescence (Lambers et al., 2009; Shirakawa et al., 2016; Zhang et al., 2024b): elevated numbers of senescent $CD28^-$ T cells have been observed in adults with chronic inflammatory diseases such as rheumatoid arthritis, COPD, and obesity (Lambers, et al., 2009; Shirakawa, et al., 2016; Bauer, 2020). However, the characteristics of T-cell senescence in asthma have not been studied in detail. In this study, we detected elevated proportions of senescent $CD4^+CD57^+CD28^-$ T cells (but not $CD8^+CD57^+CD28^-$ T cells) in the peripheral blood and sputum of asthma patients. These findings suggest that $CD4^+$ Tsens are more prevalent in asthma patients, especially in those with strong type 2 inflammation and poorly controlled asthma, than in age-matched healthy controls. Although the comparison of $CD4^+$ T-cell senescence between eosinophilic and non-eosinophilic asthma subgroups did not reach statistical significance, a trend toward higher senescence was noted in eosinophilic asthma. This apparent discrepancy with the significant increase observed in the FeNO-high group likely reflects the distinct biological nature of these biomarkers. Eosinophil counts—whether in blood or sputum—are relatively static downstream indicators of inflammation that are susceptible to modulation by corticosteroids and other external factors(Wang et al., 2023). In contrast, FeNO serves as a dynamic, real-time marker of IL-13-mediated epithelial inflammation(Escamilla-Gil et al., 2022). FeNO levels are less affected by diurnal variation or recent medication use and may better capture the current inflammatory milieu(Pelletier et al., 2022; Yuda et al., 2025). Therefore, discordance between eosinophils and FeNO is not uncommon and has been well-documented in asthma phenotyping(Badar et al., 2020). Finally, our findings were corroborated in an HDM-induced mouse model of type 2 asthma, which also exhibited increased $CD4^+$ T-cell senescence in the inflamed airway. This alignment between human and animal data supports the broader relevance of T-cell senescence as a feature of type 2 inflammatory asthma.

Our study provides important evidence that $CD4^+$ T cells in patients with type 2 asthma are more susceptible to senescence. After analysing the immune phenotypes of cells in the peripheral blood and airways in the context of asthma, we were unable to determine whether asthma induced $CD4^+$ T-cell senescence or whether senescent $CD4^+$ T cells contributed to the development of asthma. Therefore, we used an HDM-induced mouse model of asthma and found that even in young mice, asthmatic mice presented increased percentages of senescent $CD4^+$ T cells compared to PBS-treated controls. Furthermore, neutralizing IL-4 with monoclonal antibodies confirmed the causal relationship between asthma and $CD4^+$ T-cell senescence. In chronic inflammatory diseases such as asthma, long-term antigenic stimulation can lead to continuous T-cell activation and proliferation. This repeated activation may induce telomere shortening and DNA damage, impair DNA repair mechanisms, and disrupt immune modulation, ultimately leading to $CD4^+$ T-cell senescence (Mittelbrunn and Kroemer, 2021).

In addition to chronic antigenic stress, the type 2 inflammatory cytokines involved in asthma may play a key role in promoting T-cell senescence. A recent study showed that IL-4 induces senescence in human renal carcinoma cell lines through the upregulation of p21 via the STAT6 and p38 MAPK pathways (Kim et al., 2013). Another study revealed that IL-4 induces senescence in salivary epithelial cells through the ROS/p38 pathway in patients with IgG4-related sialadenitis (Min, et al., 2022). In this study, we observed that the percentage of senescent $CD4^+$ T cells in the lungs of IL-4-neutralized mice was significantly lower than that in the lungs of control mice, suggesting that type 2 inflammation contributes to $CD4^+$ T-cell senescence, with IL-4 acting as an important signalling molecule. We also confirmed the role of IL-4 and other type 2 inflammatory cytokines in inducing human $CD4^+$ T-cell senescence in vitro. Furthermore, we examined the signalling pathways involved in IL-4-induced senescence. Although both STAT6 and p38 MAPK were significantly activated in the lungs of HDM-treated mice, neutralization of IL-4 inhibited p38 MAPK activation but had no effect on STAT6 expres-

unedited

sion.

We also explored the impact of senescent $CD4^+$ T cells on asthma. Previous studies have shown that senescent $CD4^+$ T cells impair immune functions such as antiviral responses (Zhang et al., 2024a). In asthma, type 2 inflammation promotes $CD4^+$ T-cell senescence, and the generated senescent cells secrete inflammatory cytokines such as IL-1β, IL-6, IL-8, and IFN-γ, contributing to chronic inflammation (Yang et al., 2023). The SASP has been observed in elderly asthma patients and in mouse models of allergic airway inflammation (Busse et al., 2007; Busse and Mathur, 2010; Busse et al., 2017; Judge et al., 2020). In this study, we performed adoptive transfer of senescent $CD4^+$ T cells and found that while infusion of senescent $CD4^+$ T cells did not induce spontaneous asthma, it exacerbated type 2 inflammation in asthmatic mice. These findings suggest that targeting $CD4^+$ Tsens could represent a novel therapeutic approach for type 2 asthma. Our study also addresses the challenge of obtaining sufficient numbers of senescent cells from asthma patients and mice. To overcome this limitation, we induced senescence in $CD4^+$ T cells in vitro using Dox. We found that Dox-induced senescent $CD4^+$ T cells presented many typical features of senescence, but they did not fully recapitulate the characteristics of senescent $CD4^+$ T cells observed in asthma. Therefore, we plan to explore the adoptive transfer of sorted $CD4^+$ T cells expressing $CD153^+$ and $PD1^+$ from mice in future studies.

Type 2 asthma exacerbates $CD4^+$ T-cell senescence, initiating a vicious cycle of chronic inflammation. Consequently, targeting senescent $CD4^+$ T cells could be an effective asthma-treatment strategy. Currently available anti-senescence therapies, such as senomorphic and senolytic approaches, focus on targeting SASP signals to inhibit or neutralize the production of harmful SASP components or eliminate senescent cells that release these factors (Gasek et al., 2021). Drugs targeting specific senescent cell types are currently being evaluated, and senescent immune cells, particularly T cells, may be important therapeutic targets in type 2 asthma. We found that $CD153^+PD1^+CD4^+$ senescent cell abundance was increased in asthmatic mice, and previous studies have shown that a vaccine targeting senescent T cells expressing CD153 could effectively improve glucose metabolism in obese mice (Yoshida, et al., 2020; Mendelsohn and Larrick, 2022). Although CD153 has not been fully validated as a marker of senescent $CD4^+$ T cells in humans, applying antisenescence therapeutic strategies that target specific markers of senescent $CD4^+$ T cells has significant potential for the treatment of type 2 asthma.

One limitation of this study is the relatively small and imbalanced sample size between asthma patients and healthy controls, particularly in the sputum cohort, due to the invasive nature of sputum induction. To address this, we are continuing to collect clinical samples to expand the cohort, which will enable more refined subgroup analyses. Future studies with larger samples and integrated biomarker profiling will be important to validate and extend our findings. Another limitation is the lack of significant differences in $CD4^+$ T-cell senescence between eosinophil-defined asthma subgroups. While this may appear inconsistent with the elevated senescence in the high-FeNO group, it likely reflects differences in biomarker sensitivity. Eosinophil counts are downstream and easily influenced by corticosteroids, while FeNO better captures dynamic, IL-13–driven epithelial inflammation. Longitudinal studies using multiple biomarkers—such as FeNO, eosinophils, and IL-13—will help clarify the relationship between type 2 inflammation and T-cell senescence.

5 Conclusions

In this study, we demonstrated that individuals with asthma have a greater proportion of senescent $CD4^+$ T cells than healthy controls do and that the increase in $CD4^+$ Tsen abundance in asthma patients is likely mediated by type 2 inflammation. Blockade of IL-4 significantly reduced the proportion of $CD4^+$ Tsens in asthmatic mice. Moreover, adoptive transfer of senescent $CD4^+$ T cells did not induce spontaneous asthma but exacerbated type 2 inflammation. These findings highlight the therapeutic potential of targeting senescent $CD4^+$ T cells as a novel strategy for managing type 2 asthma.

unedited

Data availability statement

The data presented in this study are available from the corresponding author upon reasonable request.

Acknowledgments

This work was supported by grants from the National Natural Science Foundation of China (82370032 and 82170028), the Beijing Natural Science Foundation (7232205), the Zhong Nanshan Medical Foundation of Guangdong Province (ZNSXS-20240004), the Third Hospital of Peking University's Cohort Construction Project (BYSYDL2021020), and the Key Clinical Projects of the Third Hospital of Peking University (BYSYZD2023009) to Chun CHANG and a grant from the National Natural Science Foundation of China (81902909) to Abudureyimujiang Aili..

Author contributions

Huan LIU performed the methodology, investigation, data curation, and writing - original draft. Zemin LI performed the Investigation. Yongchang SUN contributed to the methodology, writing - review and editing. Abudureyimujiang AILI contributed to the supervision and validation. Chun CHANG contributed to the conceptualization and supervision. All authors read and approved the final manuscript and, therefore, had full access to all the data in the study and take responsibility for the integrity and security of the data.

Compliance with ethics guidelines

Huan LIU, Zemin LI, Yongchang SUN, Abudureyimujiang AILI and Chun CHANG declare that they have no conflict of interest.

All procedures followed were in accordance with the ethical standards of the responsible committee on human experimentation (Medical Science Research Ethics Committee of the Third Hospital of Peking University, Approval no. M2023075) and with the Helsinki Declaration of 1975, as revised in 2008. Informed consent was obtained from all patients for being included in the study. Additional informed consent was obtained from all patients for whom identifying information is included in this article.

unedited

Table 1 Demographics, characteristics, and clinical features of the subjects (blood donors)

Characteristic	Healthy control* (*n*=14)	Asthma* (*n*=50)	*P*-value†
Age (years)	48.14±12.30	40.26±16.61	0.104
Sex, male	6 (42.8%)	22 (44.0%)	0.939
BMI (kg/m^2)	24.12±2.96	24.18±3.61	0.960
<18.5	0 (0.0%)	3 (6.0%)	0.693
18.5-23.9	9 (64.3%)	27 (54.0%)	
24.0-27.9	4 (28.6%)	18 (36.0%)	
≥28.0	1 (7.1%)	2 (4.0%)	
Smoking history, yes	2 (14.3%)	5 (10.0%)	0.648
Acute asthma exacerbation history, yes	ND	6 (12.0%)	ND
Age of onset	ND	37.69±14.69	ND
FEV1/pred (%)	97.19±17.27	85.87±15.42	**0.038**
FEV1/FVC (%)	85.82±3.30	78.15±6.90	**0.001**
ACT	ND	19.03±4.17	ND
FeNO (ppb)	ND	74.30±53.57	ND
IgE	ND	381.97±552.21	
Eosinophils, (x10^9/L)	0.15±0.16	0.37±0.25	**0.003**
Total sputum cells, (x10^6/mL)	ND	0.88±0.75	ND
Sputum Macrophages (%)	ND	14.13±20.04	ND
Sputum Lymphocytes (%)	ND	6.10±5.73	ND
Sputum neutrophils (%)	ND	65.23±30.83	ND
Sputum eosinophils (%)	ND	14.52±22.98	ND

BMI, body mass index; FEV1, forced expiratory volume in 1 s; FVC, forced vital capacity; ACT, asthma control test; FeNO, fractional exhaled nitric oxide. ND, not determined

* Continuous variables are presented as the means±standard deviations (SD); categorical variables are shown as *n* (%).

† *P* values were derived using *t* tests for continuous data and χ^2 tests for categorical data.

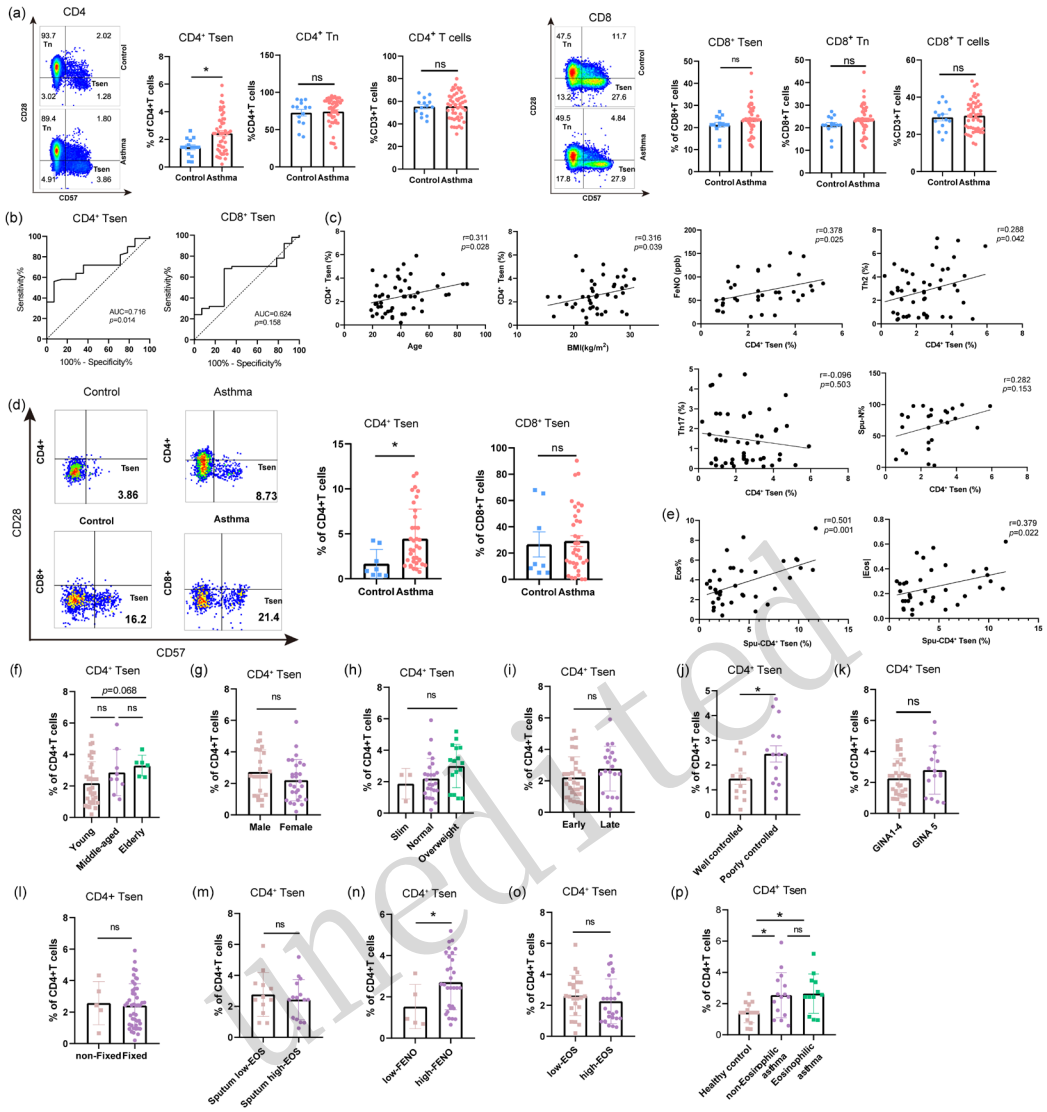

Fig. 1 Increased abundance of CD4$^+$ Tsens in patients with asthma. (a) Representative flow-cytometry plots and statistical analysis of the percentages of total CD4$^+$ T cells, total CD8$^+$ T cells, the CD28$^+$CD57$^-$ non-senescent T cell (Tn) subset, and the CD28$^-$CD57$^+$ senescent T-cell (Tsens) subset in the blood of patients with asthma (n=50) compared with healthy controls (n=14). Bars show the means with standard errors of the means. (b) ROC curve of CD4$^+$ Tsen and CD8$^+$ Tsen percentages in patients with asthma and healthy controls. (c) Correlations between the percentage of CD4$^+$ Tsens in the blood and age, BMI, FeNO values, percentage of Th2 cells and Th17 cells, and sputum neutrophil ratio. (d) Representative flow-cytometry plots and statistical analysis showing the percentages of the CD28$^+$CD57$^-$ (Tn) and CD28$^-$CD57$^+$ (Tsen) subsets for CD4$^+$ T and CD8$^+$ T cells in sputum from patients with asthma (n=36) compared with healthy controls (n=8). (e) Correlations between the percentage of CD4$^+$ Tsens in sputum and the cell counts and percentages of eosinophils in the blood. Percentages of CD4$^+$ Tsens: (f) in patients of different ages. (g) in male and female patients. (h) in patients with different BMIs. (i) in patients with different ages of onset. (j) in patients with well controlled (ACT>20) and poorly controlled (ACT<20) asthma. (k) in patients at the GINA1-4 and GINA5 treatment stages. (l) in patients with fixed airflow limitation and nonfixed airflow limitation. (m) in patients with high sputum eosinophil counts (sputum eosinophil ratio > 2%) and low sputum eosinophil counts (sputum eosinophil ratio ≤2%). (n) in patients with FeNO > 20 ppb and FeNO < 20 ppb. (o) in patients with hypereosinophilia (eosinophils ≥150 cells/μL) and hypoeosinophilia (eosinophils <150 cells/μL). (p) in patients with eosinophilic asthma (sputum eosinophil ratio≥3% and sputum neutrophil ratio <61%) and non-eosinophilic asthma (sputum eosinophil ratio <3%). Correlation analysis was performed using Spearman's rank correlation coefficient. Data from different groups were statistically analyzed using t tests and analyses of variance. Bars show means with standard errors of the means. * P < 0.05; ns, P > 0.05. Abbreviations: BMI, body mass index; FeNO, fractional exhaled nitric oxide; Th2/Th17/Th1, T helper …; ACT, Asthma Control Test; ROC, receiver operating characteristic; ns, not significant.

Unedited

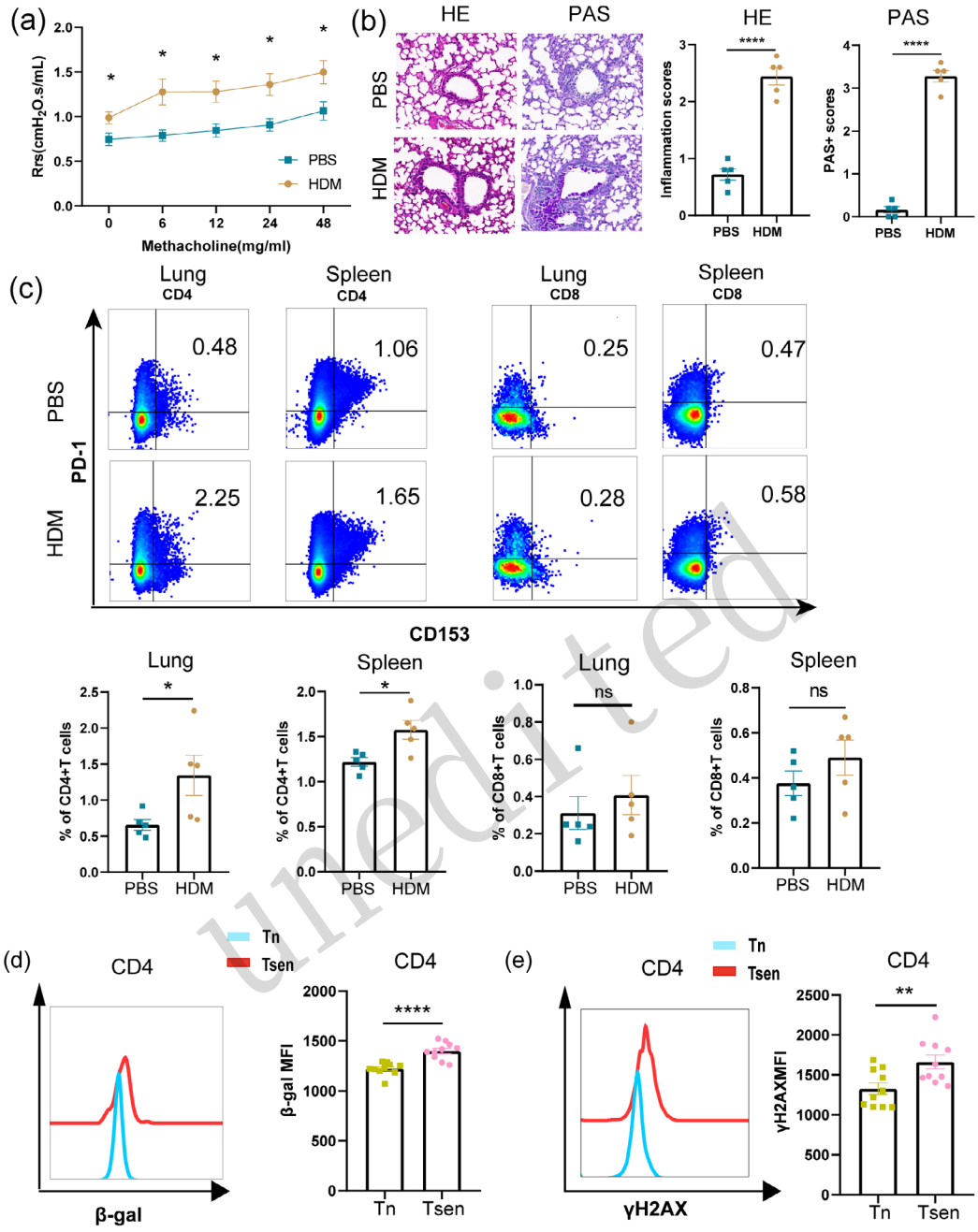

Fig. 2 Increased CD4+ Tsen abundance in mice with asthma

(a) Total resistance of the respiratory system in mice treated with increasing concentrations of methacholine (0–48 mg/mL). (b) Representative images of HE- and PAS-stained lung sections from each group (images were captured at 400× magnification; scale bar = 20 μm). (c) Representative flow-cytometry plots and statistical analysis of percentages of the $CD153^{-}PD1^{-}$ (Tn) and $CD153^{+}PD1^{+}$ (Tsen) subsets among $CD4^{+}$ T cells and $CD8^{+}$ T cells in the lungs and spleens of mice with asthma compared with controls (n = 5). (d) Representative flow-cytometry plots and statistical analysis of the MFI of SA-β-Gal activity (n = 5). (e) Representative flow-cytometry plots and statistical analysis of the MFI of γ-H2AX (n = 5). Data from different groups were statistically analyzed via t tests. The bars show the means with standard errors of the means. *, $P < 0.05$; **, $P < 0.01$; ***, $P < 0.001$; ****, $P < 0.0001$; ns, $P > 0.05$. Abbreviations: hematoxylin & eosin (HE); periodic acid–Schiff (PAS); mean fluorescence intensity (MFI).

unedited

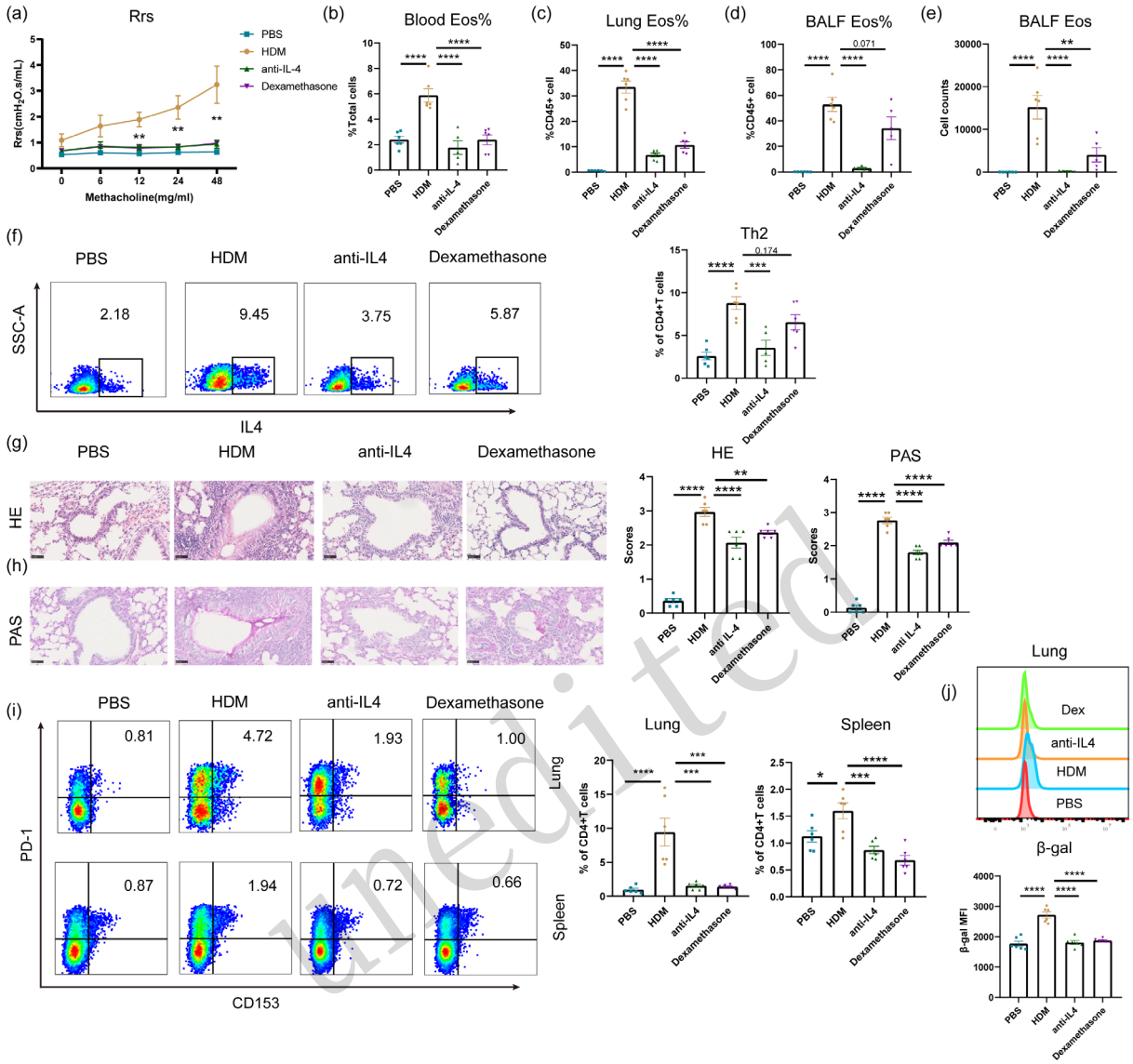

Fig. 3 Ability of IL-4 antibody and dexamethasone injection to exert therapeutic effects by preventing senescent CD4$^+$ T-cell accumulation and type 2 inflammation in mice with asthma

(a) Total resistance of the respiratory system of mice treated with increasing concentrations of methacholine (0–48 mg/mL). (b-e) Statistical analysis of percentages of eosinophils in the blood (b), lungs (c), and BALF (d) and cell counts of eosinophils (e) in mouse BALF. (f) Representative flow-cytometry plots and statistical analysis showing percentages of Th2 cells in mouse lungs. (g, h) Representative images of HE- and PAS-stained lung sections from each group (images were captured at 400× magnification; scale bars = 50 μm). (i) Representative flow-cytometry plots and statistical analysis showing percentages of CD153$^+$PD1$^+$CD4$^+$ T cells (Tsens) in mouse lungs and spleens (n = 6). (j) Representative flow-cytometry plots and statistical analysis of the MFI of SA-β-Gal activity in CD4$^+$ T cells in mouse lungs. Statistical significance was determined in comparison with the asthma group. *, $P < 0.05$; **, $P < 0.01$; ***, $P < 0.001$; ****, $P < 0.0001$; ns, $P > 0.05$. Abbreviations: Bronchoalveolar Lavage Fluid (BALF); T helper 2 (Th2); Senescence-Associated β-Galactosidase (SA-β-Gal).

unedited

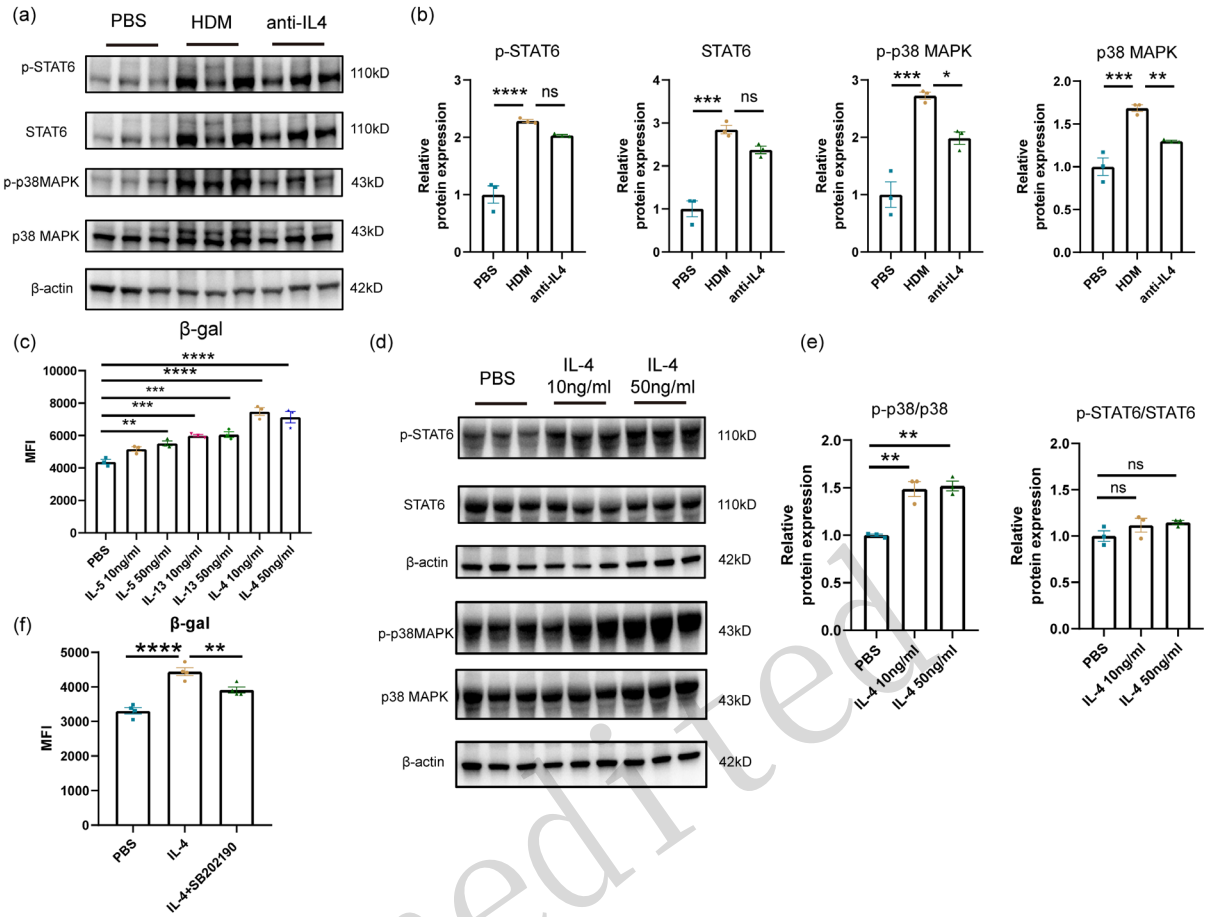

Fig. 4 The type 2 inflammatory cytokine IL-4 induces senescence in CD4$^+$ T cells

(a, b) Western blot and quantification of the phosphorylation and total protein of p38 MAPK and STAT6 in lungs of mice (n=3) treated with PBS, HDM, and HDM + IL-4 antibody. Statistical significance was determined in comparison with the asthma group. (c) Senescence-induction effects of different concentrations of IL-4, IL-5, and IL-13 in human CD4$^+$ T cells. (d, e) Western blot and quantification of the phosphorylation and total protein of p38 MAPK and STAT6 in human CD4$^+$ T cells treated with PBS or IL-4 (n = 3). (f) Statistical diagram of the MFI of SA-β-Gal activity in human CD4$^+$ T cells treated with IL-4 or IL-4 combined with SB202190 (n = 4). *, $P < 0.05$; **, $P < 0.01$; ***, $P < 0.001$; ****, $P < 0.0001$; ns, $P > 0.05$. Abbreviations: interleukin-4 (IL-4); signal transducer and activator of transcription 6 (STAT6); p38 mitogen-activated protein kinase (p38 MAPK).

unedited

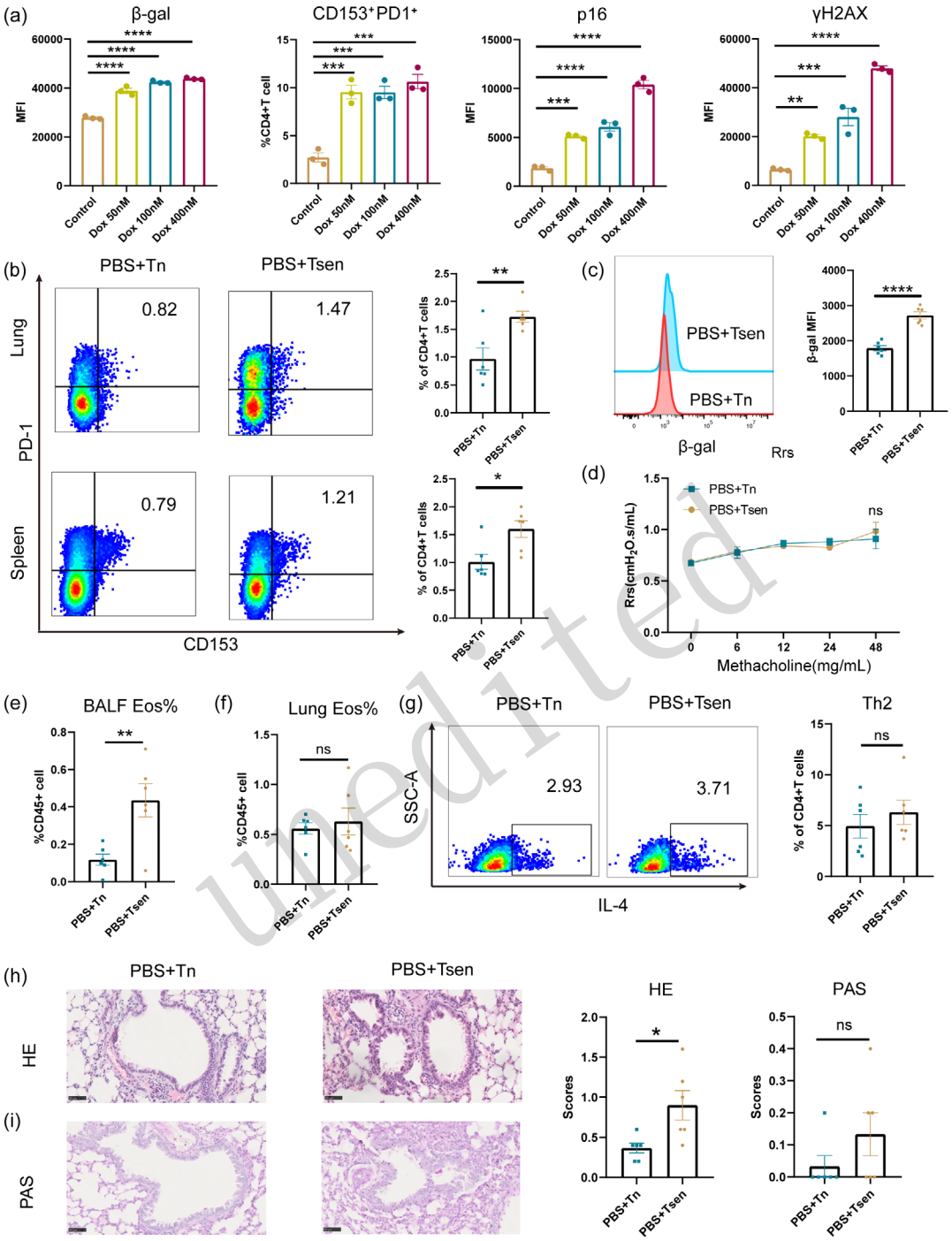

Fig. 5 Adoptive transfer of senescent CD4⁺ T cells in healthy mice does not induce spontaneous asthma onset

(a) Senescence-induction effect of doxorubicin (Dox) at different concentrations in CD4⁺ T cells. (b, c) Representative flow-cytometry plots and statistical analysis showing percentages of CD153⁺PD1⁺CD4⁺ T cells (Tsens) and the MFI of SA-β-Gal activity in CD4⁺ T cells in mouse lungs and spleens (n = 6). (d) Total resistance of respiratory system in mice treated with increasing concentrations of methacholine (0–48 mg/mL). (e-f) Statistical analysis of percentages of eosinophils in the BALF (e) and lungs (f) of mice. (g) Representative flow-cytometry plots and statistical analysis of the percentages of Th2 cells in mouse lungs. (h, i) Representative images of HE- and PAS-stained lung sections from each group (images were captured at 400× magnification; scale bars = 50 μm). Statistical significance was assessed in comparison to the Tn group. *, $P < 0.05$; **, $P < 0.01$; ***, $P < 0.001$; ****, $P < 0.0001$; ns, $P > 0.05$.

unedited

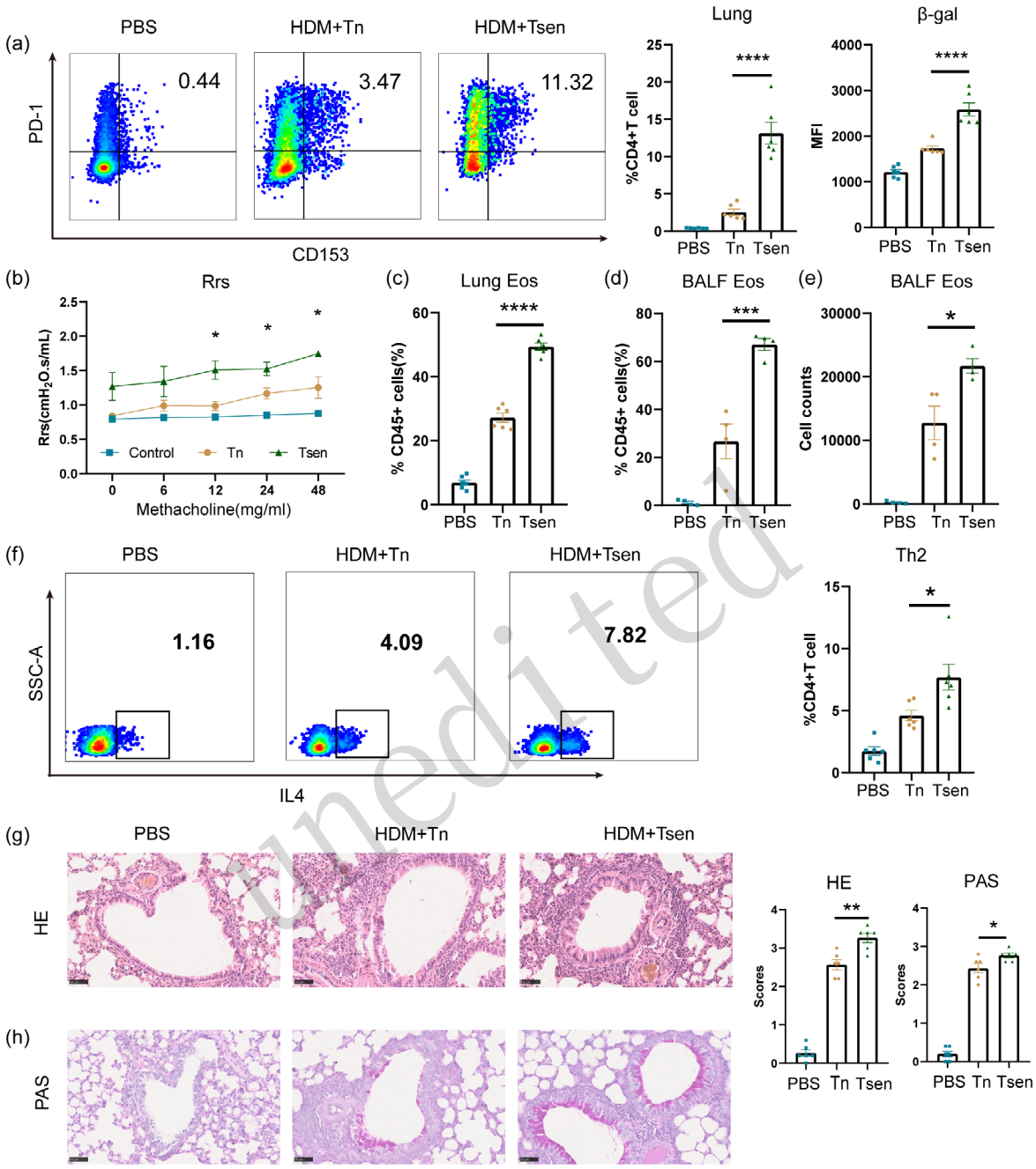

unedited

Fig. 6 Adoptive transfer of senescent CD4+ T cells promotes type 2 inflammation in HDM-treated mice
(a) Representative flow-cytometry plots and statistical analysis of percentages of $CD153^+PD1^+CD4^+$ T cells (Tsens) and the MFI of SA-β-Gal activity in $CD4^+$ T cells in mouse lungs (n = 6). (b) Total resistance of the respiratory system in mice treated with increasing concentrations of methacholine (0–48 mg/mL). (c-e) Statistical analysis of the percentages of eosinophils in the lungs (c) and BALF (d) and the number of eosinophils (e) in the BALF of mice. (f) Representative flow-cytometry plots and statistical analysis of the percentages of Th2 cells in mouse lungs of the mice. (g, h) Representative images of HE- and PAS-stained lung sections from each group (images were captured at 400× magnification; scale bars = 50 μm). Statistical significance was assessed in comparison to the Tn group. *, $P < 0.05$; **, $P < 0.01$; ***, $P < 0.001$; ****, $P < 0.0001$; ns, $P > 0.05$.

References

Aghali A, Khalfaoui L, Lagnado AB, et al., 2022. Cellular senescence is increased in airway smooth muscle cells of elderly persons with asthma. *Am J Physiol Lung Cell Mol Physiol*, 323(5):L558-l568. https://doi.org/10.1152/ajplung.00146.2022

Akbar AN, Henson SM, Lanna A, 2016. Senescence of t lymphocytes: Implications for enhancing human immunity. *Trends Immunol*, 37(12):866-876. https://doi.org/10.1016/j.it.2016.09.002

Badar A, Salem AM, Bamosa AO, et al., 2020. Association between feno, total blood ige, peripheral blood eosinophil and inflammatory cytokines in partly controlled asthma. *J Asthma Allergy*, 13:533-543. https://doi.org/10.2147/jaa.S274022

Bauer ME, 2020. Accelerated immunosenescence in rheumatoid arthritis: Impact on clinical progression. *Immun Ageing*, 17:6. https://doi.org/10.1186/s12979-020-00178-w

Busse PJ, Zhang TF, Srivastava K, et al., 2007. Effect of ageing on pulmonary inflammation, airway hyperresponsiveness and t and b cell responses in antigen-sensitized and -challenged mice. *Clin Exp Allergy*, 37(9):1392-1403. https://doi.org/10.1111/j.1365-2222.2007.02775.x

Busse PJ, Mathur SK, 2010. Age-related changes in immune function: Effect on airway inflammation. *J Allergy Clin Immunol*, 126(4):690-699; quiz 700-691. https://doi.org/10.1016/j.jaci.2010.08.011

Busse PJ, Birmingham JM, Calatroni A, et al., 2017. Effect of aging on sputum inflammation and asthma control. *J Allergy Clin Immunol*, 139(6):1808-1818.e1806. https://doi.org/10.1016/j.jaci.2016.09.015

Childs BG, Durik M, Baker DJ, et al., 2015. Cellular senescence in aging and age-related disease: From mechanisms to therapy. *Nat Med*, 21(12):1424-1435. https://doi.org/10.1038/nm.4000

Childs BG, Gluscevic M, Baker DJ, et al., 2017. Senescent cells: An emerging target for diseases of ageing. *Nat Rev Drug Discov*, 16(10):718-735. https://doi.org/10.1038/nrd.2017.116

Collaborators GCRD, 2020. Prevalence and attributable health burden of chronic respiratory diseases, 1990-2017: A systematic analysis for the global burden of disease study 2017. *Lancet Respir Med*, 8(6):585-596. https://doi.org/10.1016/s2213-2600(20)30105-3

Devulder JV, 2024. Unveiling mechanisms of lung aging in copd: A promising target for therapeutics development. *Chin Med J Pulm Crit Care Med*, 2(3):133-141. https://doi.org/10.1016/j.pccm.2024.08.007

Escamilla-Gil JM, Fernandez-Nieto M, Acevedo N, 2022. Understanding the cellular sources of the fractional exhaled nitric oxide (feno) and its role as a biomarker of type 2 inflammation in asthma. *Biomed Res Int*, 2022:5753524. https://doi.org/10.1155/2022/5753524

Gasek NS, Kuchel GA, Kirkland JL, et al., 2021. Strategies for targeting senescent cells in human disease. *Nat Aging*, 1(10):870-879. https://doi.org/10.1038/s43587-021-00121-8

Global initiative for asthma (GINA). *2023 GINA Report*.. Global strategy for asthma management and prevention. Available from http://www.ginasthma.org

Gorgoulis V, Adams PD, Alimonti A, et al., 2019. Cellular senescence: Defining a path forward. *Cell*, 179(4):813-827. https://doi.org/10.1016/j.cell.2019.10.005

Hammad H, Lambrecht BN, 2021. The basic immunology of asthma. *Cell*, 184(9):2521-2522. https://doi.org/10.1016/j.cell.2021.04.019

Huang K, Yang T, Xu J, et al., 2019. Prevalence, risk factors, and management of asthma in china: A national cross-sectional study. *Lancet*, 394(10196):407-418. https://doi.org/10.1016/s0140-6736(19)31147-x

Judge SJ, Murphy WJ, Canter RJ, 2020. Characterizing the dysfunctional nk cell: Assessing the clinical relevance of exhaustion, anergy, and senescence. *Front Cell Infect Microbiol*, 10:49. https://doi.org/10.3389/fcimb.2020.00049

Kalidhindi RSR, Ambhore NS, Balraj P, et al., 2021. Androgen receptor activation alleviates airway hyperresponsiveness, inflammation, and remodeling in a murine model of asthma. *Am J Physiol Lung Cell Mol Physiol*, 320(5):L803-l818. https://doi.org/10.1152/ajplung.00441.2020

Kim HD, Yu SJ, Kim HS, et al., 2013. Interleukin-4 induces senescence in human renal carcinoma cell lines through stat6 and p38 mapk. *J Biol Chem*, 288(40):28743-28754. https://doi.org/10.1074/jbc.M113.499053

Lambers C, Hacker S, Posch M, et al., 2009. T cell senescence and contraction of t cell repertoire diversity in patients with chronic obstructive pulmonary disease. *Clin Exp Immunol*, 155(3):466-475. https://doi.org/10.1111/j.1365-2249.2008.03835.x

López-Otín C, Blasco MA, Partridge L, et al., 2023. Hallmarks of aging: An expanding universe. *Cell*, 186(2):243-278. https://doi.org/10.1016/j.cell.2022.11.001

Madruga MP, Grun LK, Santos L, et al., 2024. Excess of body weight is associated with accelerated t-cell senescence in hospitalized covid-19 patients. *Immun Ageing*, 21(1):17. https://doi.org/10.1186/s12979-024-00423-6

Mendelsohn AR, Larrick JW, 2022. Antiaging vaccines targeting senescent cells. *Rejuvenation Res*, 25(1):39-45. https://doi.org/10.1089/rej.2022.0008

Min SN, Zhu MQ, Mao XD, et al., 2022. Contribution of interleukin-4-induced epithelial cell senescence to glandular fibrosis in igg4-related sialadenitis. *Arthritis Rheumatol*, 74(6):1070-1082. https://doi.org/10.1002/art.42052

Mittelbrunn M, Kroemer G, 2021. Hallmarks of t cell aging. *Nat Immunol*, 22(6):687-698. https://doi.org/10.1038/s41590-021-00927-z

Nakagami Y, Favoreto S, Jr., Zhen G, et al., 2008. The epithelial anion transporter pendrin is induced by allergy and rhinovirus infection, regulates airway surface liquid, and increases airway reactivity and inflammation in an asthma model. *J Immunol*, 181(3):2203-2210. https://doi.org/10.4049/jimmunol.181.3.2203

Ödling M, Andersson N, Ekström S, et al., 2018. Characterization of asthma in the adolescent population. *Allergy*,

Unedited

73(8):1744-1746. https://doi.org/10.1111/all.13469
Pelletier G, Godbout K, Boulay M, et al., 2022. Increase in feno levels following il5/il5r-targeting therapies in severe asthma: A case series. *J Asthma Allergy*, 15:691-701. https://doi.org/10.2147/jaa.S358877
Schafer MJ, White TA, Iijima K, et al., 2017. Cellular senescence mediates fibrotic pulmonary disease. *Nat Commun*, 8:14532. https://doi.org/10.1038/ncomms14532
Shirakawa K, Yan X, Shinmura K, et al., 2016. Obesity accelerates t cell senescence in murine visceral adipose tissue. *J Clin Invest*, 126(12):4626-4639. https://doi.org/10.1172/jci88606
Soma T, Nagata M, 2022. Immunosenescence, inflammaging, and lung senescence in asthma in the elderly. *Biomolecules*, 12(10) https://doi.org/10.3390/biom12101456
Sturmlechner I, Zhang C, Sine CC, et al., 2021. P21 produces a bioactive secretome that places stressed cells under immunosurveillance. *Science*, 374(6567):eabb3420. https://doi.org/10.1126/science.abb3420
Tibbitt CA, Stark JM, Martens L, et al., 2019. Single-cell rna sequencing of the t helper cell response to house dust mites defines a distinct gene expression signature in airway th2 cells. *Immunity*, 51(1):169-184.e165. https://doi.org/10.1016/j.immuni.2019.05.014
Wan R, Srikaram P, Guntupalli V, et al., 2023. Cellular senescence in asthma: From pathogenesis to therapeutic challenges. *EBioMedicine*, 94:104717. https://doi.org/10.1016/j.ebiom.2023.104717
Wang K, Stonham C, Rutherford C, et al., 2023. Fractional exhaled nitric oxide (feno): The future of asthma care? *Br J Gen Pract*, 73(737):565-568. https://doi.org/10.3399/bjgp23X735813
Wang TW, Johmura Y, Suzuki N, et al., 2022. Blocking pd-l1-pd-1 improves senescence surveillance and ageing phenotypes. *Nature*, 611(7935):358-364. https://doi.org/10.1038/s41586-022-05388-4
Wang ZN, Su RN, Yang BY, et al., 2020. Potential role of cellular senescence in asthma. *Front Cell Dev Biol*, 8:59. https://doi.org/10.3389/fcell.2020.00059
Weyand CM, Yang Z, Goronzy JJ, 2014. T-cell aging in rheumatoid arthritis. *Curr Opin Rheumatol*, 26(1):93-100. https://doi.org/10.1097/bor.0000000000000011
Wood WA, Krishnamurthy J, Mitin N, et al., 2016. Chemotherapy and stem cell transplantation increase p16(ink4a) expression, a biomarker of t-cell aging. *EBioMedicine*, 11:227-238. https://doi.org/10.1016/j.ebiom.2016.08.029
Yang J, Liu HC, Zhang JQ, et al., 2023. The effect of metformin on senescence of t lymphocytes. *Immun Ageing*, 20(1):73. https://doi.org/10.1186/s12979-023-00394-0
Yoshida S, Nakagami H, Hayashi H, et al., 2020. The cd153 vaccine is a senotherapeutic option for preventing the accumulation of senescent t cells in mice. *Nat Commun*, 11(1):2482. https://doi.org/10.1038/s41467-020-16347-w
Yuda E, Ando T, Ishida Y, et al., 2025. Investigation of individual variability and temporal fluctuations in exhaled nitric oxide (feno) levels in healthy individuals. *Adv Respir Med*, 93(4) https://doi.org/10.3390/arm93040026
Zhang J, Chang C, Liang Z, et al., 2024a. Elevated cd4(+) t cell senescence associates with impaired immune responsiveness in severe covid-19. *Aging Dis*, https://doi.org/10.14336/ad.2024.0214-2
Zhang M, Lin J, Zhang J, et al., 2023. Artesunate inhibits airway remodeling in asthma via the mapk signaling pathway. *Front Pharmacol*, 14:1145188. https://doi.org/10.3389/fphar.2023.1145188
Zhang P, Catterson JH, Grönke S, et al., 2024b. Inhibition of s6k lowers age-related inflammation and increases lifespan through the endolysosomal system. *Nat Aging*, 4(4):491-509. https://doi.org/10.1038/s43587-024-00578-3

unedited

Supplementary information:
Table S1-S5 and Figs. S1-S7